Journal of Machine Engineering, Vol. 13, No. 3, 2013

damping, linear rolling bearing,
response function, dynamic

Yasunori SAKAI[1]
Masaomi TSUTSUMI[2]

DYNAMIC CHARACTERISTICS OF LINEAR ROLLING BEARINGS FOR MACHINE TOOLS

The present paper proposes a method for evaluating the dynamic characteristics of a single linear rolling bearing subjected to a radial force and a bending moment. In order to evaluate the damping of a rail-carriage system, a rectangular column with a flange is fixed to the carriage by bolts, and the free end of the column is excited by an impulse hammer in the horizontal (x), lateral (y), and radial (z) directions. The response is detected by an accelerometer mounted to the flange of the column. Both force and acceleration are input to an FFT analyzer, and the frequency response function (FRF) is calculated. The damping capacity in each direction is evaluated as a modal damping ratio, which is calculated based on the FRF. As a result, the damping ratio of the vibration mode in the feed (x) direction is higher than those of the other vibration modes. In addition, the influence of the nonlinearity of the linear rolling bearings on the dynamic characteristics is investigated. The results reveal that the dynamic characteristics of the linear rolling bearings depend on the excitation direction.

1. INTRODUCTION

Linear rolling bearings with low friction and high accuracy are suitable for guideways for high-speed, high-precision feed drive mechanisms and are widely used in machine tools. When rolling bearings are applied to guideways, which are standardized in an ISO standard [1], they facilitate the design, assembly and maintenance of machine tools. Thus, linear rolling bearings are essential in the feed drive mechanism. However, the linear rolling bearings of guideways of machine tools are gradually being replaced by sliding bearings, which have high damping capacity. The high damping capacity of sliding bearings is desirable because the chatter vibration in the machining process can be avoided if the guideway has high damping capacity.

Numerous studies on linear rolling guideways have examined the life distribution and reliability of roller-based linear rolling bearings [2],[3] the sound and vibration of the recirculating linear ball bearings [4], and the dynamic analysis of a single carriage of linear rolling bearings [5]. Experimental and simulation results have demonstrated that the

[1] Tokyo Institute of Technology, Department of Mechanical and Control Engineering
[2] Tokyo University of Agriculture and Technology, Institute of Engineering

damping capacity of a sliding bearing is higher than that of a linear rolling bearing and that chatter vibration can be prevented by increasing the damping capacity of the guideways. Bode [6] invented a damping element which is contacted with a rail and that can increase the damping capacity of a linear bearing. Rahman et al. [7] tried to improve the damping capacity of the feed drive mechanism using a damping carriage constructed of polymer concrete. Powalka et al. [8] attempted to improve the damping capacity of a linear rolling bearing by sandwiching resin thin films between the rail and the base. Although the damping capacity of feed drive mechanisms has been evaluated, the damping capacity of a single linear rolling bearing was not discussed in the above studies.

Several methods for evaluating the damping capacity of a single linear rolling bearing have been proposed by IKO [9], NSK [10], and Brecher et al. [11]. IKO and NSK conducted experiments to measure the damping capacity of a single linear rolling bearing using a dedicated jig that was fixed to a base by means of bolts. Figure 1 shows the typical experimental setup for measuring the damping of the linear rolling bearings. As shown in this figure, a linear rolling bearing was excited using an impulse hammer parallel to the feed direction and the damping ratio is calculated from the impulse response of the acceleration detected by an accelerometer mounted to the side of the jig. IKO showed that the free vibration curve of a roller-based linear rolling bearing decays faster than that of a linear ball bearing [9]. NSK showed that the damping capacity of a linear ball bearing increases with increasing preload [10]. However, the fixed conditions of the jig shown in Fig. 1 may affect the vibration damping of the linear ball bearing because the bolted joint used to fix the jig to the base may govern the measured damping. On the other hand, Brecher et al. evaluated the damping ratio of a roller-based linear rolling bearing through comparison with a reference dummy with comparable stiffness to that of the test rolling linear bearing [11]. They determined the damping ratio by comparing the frequency response function (FRF) of a linear rolling bearing and its reference dummy shown in Fig. 2. They showed that the damping ratio of the linear rolling bearing depends on the preload in the radial direction and yaw direction. However, this is an indirect method of measuring the damping ratio because they compared two test results.

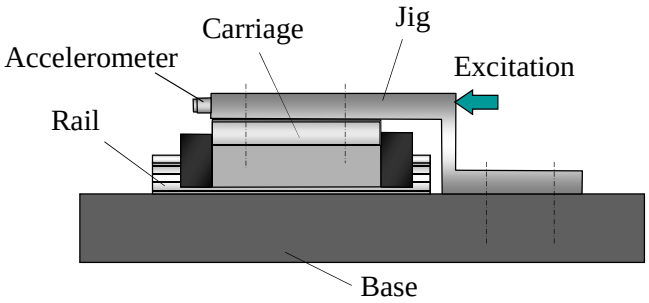

Fig. 1. Experimental setup for measuring the damping of a single linear guide (http://www.jp.nsk.com/services/pm_techreport/report40.html)

As mentioned above, only two methods to determine the damping ratio of linear rolling bearings have been reported. However, it is necessary to determine the damping ratios in three directions in order to apply the measured damping ratios to the analysis of the

dynamic performance of machine tools. A method of measuring the damping ratios of a linear rolling bearing that is not affected by the fixed conditions of the test jig must be developed.

The present paper proposes a method for directly evaluating the dynamic characteristics of a single linear rolling bearing. This method can evaluate the dynamic characteristics of a linear rolling bearing under bending moments by using a column. The column is not fixed on the surfaces excluding the top surface of a carriage. Thus the evaluated dynamic characteristics are not influenced by the boundary conditions. The FRF of a linear rolling bearing is measured using the impulse response method, and the damping capacity is evaluated based on the modal damping ratio, which is calculated based on an FRF. The evaluation results indicate that there is a direction dependency in the dynamic characteristics of a linear rolling bearing. The reason for the existence of this direction dependency was investigated. Since the carriage of a linear rolling bearing is supported by rolling elements, Hertzian contact is generated between the raceways and rolling elements. Therefore, nonlinearity is considered to exist in the vibration characteristic of a linear rolling bearing. The relationship between the dynamic characteristic and the magnitude of the excitation force is examined, and the results indicate that the nonlinearity of the linear rolling bearing influences its dynamic characteristics.

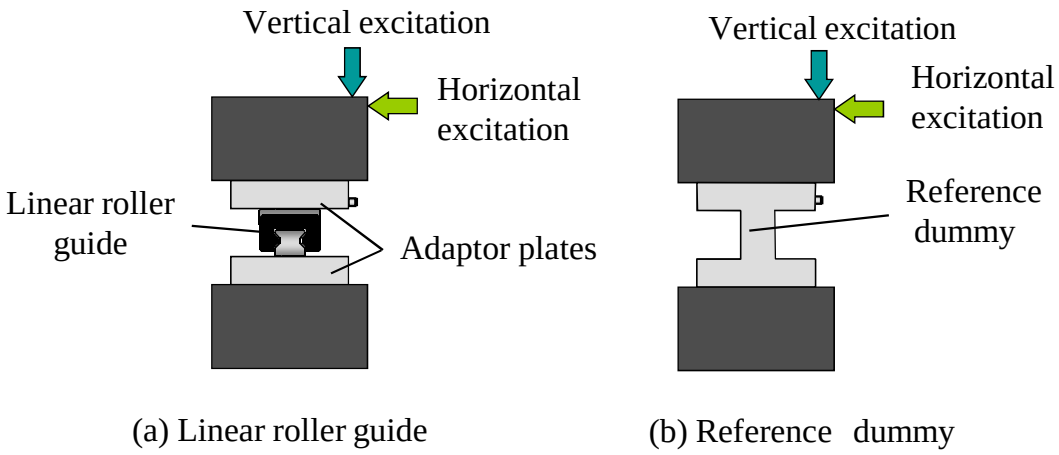

Fig. 2. Experimental setup used by Brecher et al. [11]

2. EXPERIMENTAL SETUP

A column used to measure the dynamic characteristics is tightly fixed to the top surface of the carriage of a linear rolling bearing by means of six bolts. The column applies the bending moment and the radial force to the carriage. Figure 3 shows the experimental setup for measuring the dynamic characteristics. The dimensions of the linear rolling bearing and column are also shown in Fig. 3. An LRXDG35 roller-based linear rolling bearing (preload grade: T2) (IKO Nippon Thompson Co., Ltd.) was used for the experiment.

The T2 preload grade, which is also referred to as medium preload grade, is generally chosen for machine tools. The carriage, rail, and rollers were washed with kerosene so that the lubricant oil film on the raceway would not influence the dynamic characteristics of the linear rolling bearing. The column was bolted to the top surface of the carriage by means of a long stick wrench.

The column was excited in the *x* and *y* directions as shown in Fig. 3 in order to apply the bending moment to the carriage and was excited in the *z* direction in order to apply the radial force to the carriage. While applying the bending moment and radial force to the

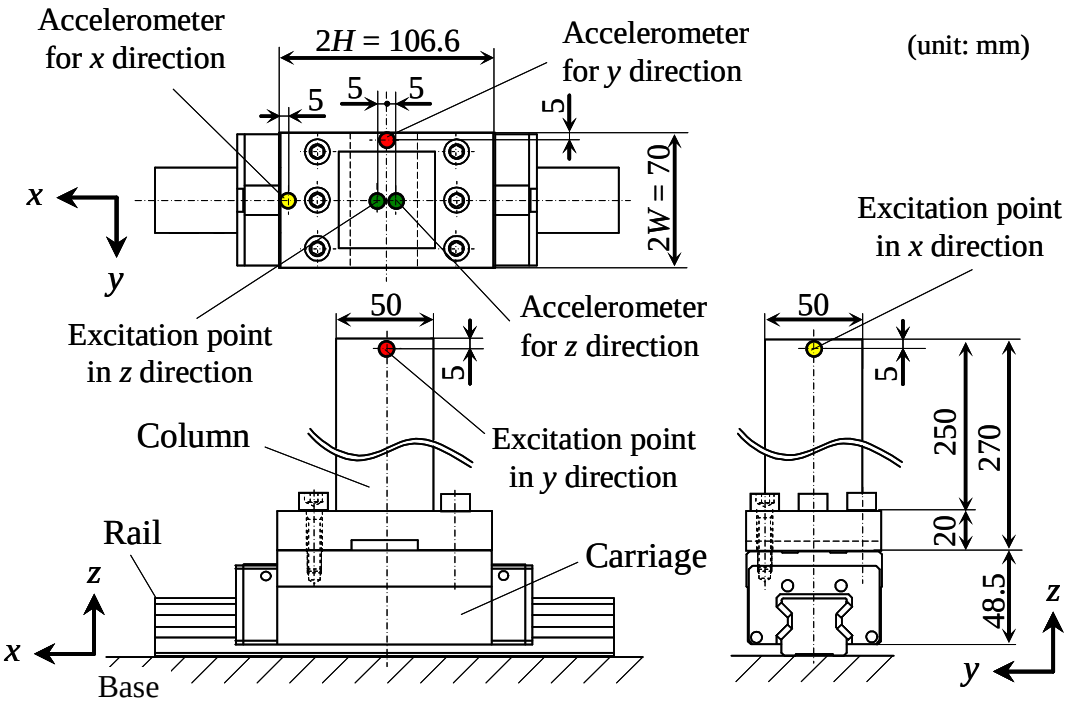

Fig. 3. Schematic illustration of experimental setup (unit: mm)

carriage, the FRF between the top of the column and the top surface of the carriage was measured. Some resonance peaks exist in the measured FRFs, and the modal damping ratios in each resonance peak were calculated to evaluate the damping capacity of a linear rolling bearing. Figure 4 shows the experimental setup for measuring an FRF between the top of the column and the top surface of the carriage of a linear rolling bearing. As shown in Fig. 4, the rail is fixed to the base by bolts, and the base is fixed to a stone surface plate (mass: 540kg, length: 1,000mm, width: 1,000mm, and height: 180mm), which is supported by air dampers. Since the mass of the stone surface plate is greater than that of the carriage, the stone surface plate can be assumed to be a rigid body. Since the stone surface plate is supported by air dampers, the experimental setup can be isolated from floor vibration. Moreover, since the base is designed for use in a feed drive mechanism, two rails can be mounted to the base. However, one rail and the carriages, which are not needed for measurement, are removed from the base in order to simplify the experimental setup. Figure 5 shows the FRF measurement system.

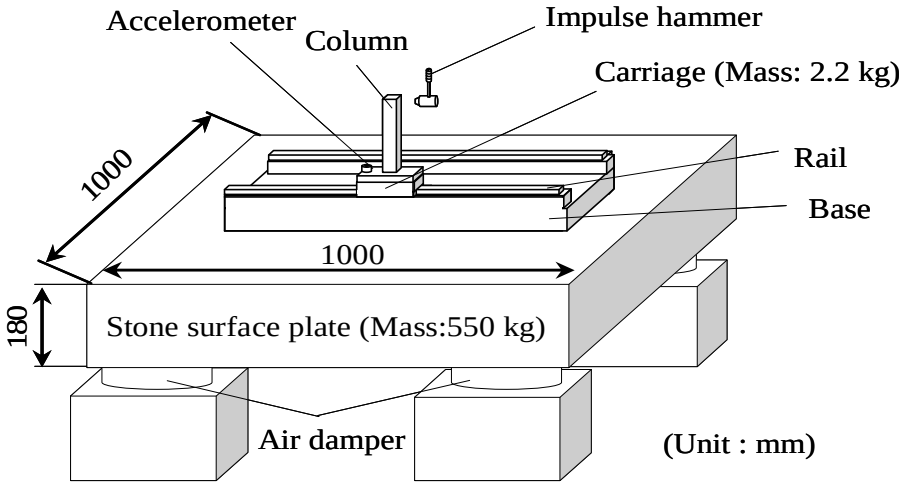

Fig. 4. Experimental setup for measuring frequency response function

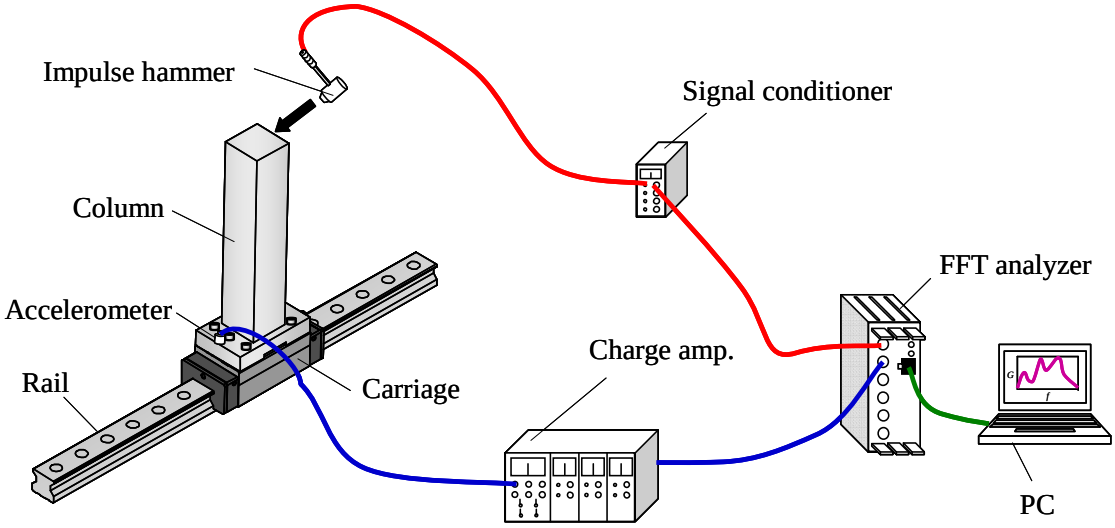

Fig. 5. Measuring system of frequency response

The FRF between the top of the column and the top surface of the carriage is calculated based on the excitation force generated by an impulse hammer and the acceleration detected by an accelerometer mounted to the top surface of the carriage. The excitation force is detected by a force transducer built into an impulse hammer. The accelerometer is mounted in the location in which the response amplitude is largest in the excitation direction. The excitation points and detection points for each direction are shown in Fig. 3. Output signals detected by a force transducer and an accelerometer are input to an FFT analyzer through a signal conditioner and a charge amplifier, respectively. An FRF is output from an FFT analyzer to a personal computer (PC). The FRF averaged 16 times in the frequency domain is used to evaluate the damping ratio of a linear rolling bearing. Therefore, the number of averaging is set to be 16. As will be discussed later, the

dynamic characteristic of a linear rolling bearing changes with the magnitude of an excitation force. Thus, the magnitude of the excitation force remains small.

In machine tools, the carriage is fixed in the *x* direction by the ball screw or linear motor with the control system in practice. And it influences on the dynamic characteristics of the linear rolling bearing. For excluding the influence of the ball screw, the linear motor and the control system, the *x* direction is not fixed.

3. VIBRATION OF LINEAR ROLLING BEARINGS

3.1. FREQUENCY RESPONSE

The FRFs generated when forces are applied in the *x*, *y*, and *z* directions are shown in Fig. 6. The FRFs are displayed as Bode diagrams. The phase is shown from -180° to 180°, and the compliance is shown on a logarithm scale.

As shown in Fig. 6a, predominant peaks appear at 0.6 and 2.6kHz when the excitation force is applied in the *x* direction. In the following, the vibration modes in the x direction are referred to as the first and second modes in order of increasing frequency.

As shown in Fig. 6b, predominant peaks appear at 0.2, 1.5, and 1.6kHz when the excitation force is applied in the *y* direction. In the following, the vibration modes in the *y* direction are referred to as the first through third modes in order of increasing frequency. Since the second mode and third mode exist in adjacent frequencies, the possibility exists that one resonance peak was divided into two peaks.

Figure 6c shows that predominant peaks appear at 1.1, 2.0, 2.1, 2.3, and 2.5kHz when the excitation force is applied in the *z* direction. In the following, the vibration modes in the *z* direction are referred to as the first through fifth modes in order of increasing frequency.

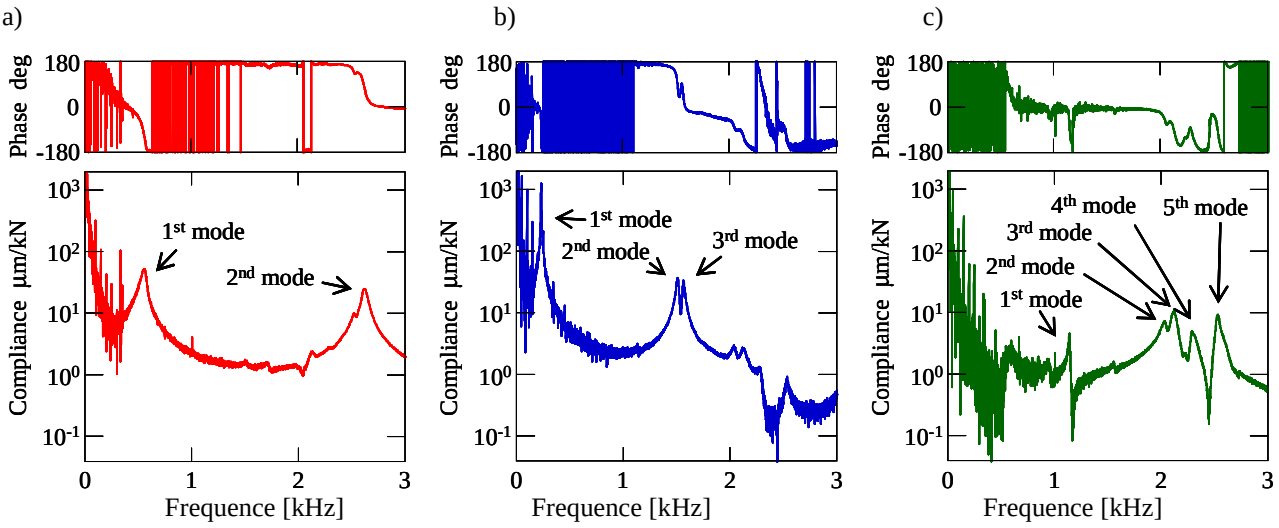

Fig. 6. Frequency response function in each excitation direction: a) x direction, b) y direction, c) z direction

3.2. MODE SHAPES

The mode shape of the carriage to which the column is fixed is measured using an experimental modal analysis method in order to clarify the vibration state when the carriage is excited in each direction. The mode shapes are measured by reading the amplitude and phase of an FRF. Although the excitation point is fixed for each direction as shown in Fig. 3, the detection point of acceleration is varied as shown in Fig. 7. A single-axis accelerometer is replaced on each detection point.

In order to measure the mode shapes of the top surface of the carriage, accelerometers are attached in a reticular pattern on the flange of the column at nine points. In order to measure the mode shapes of the side surface of the column and carriage, accelerometers are attached to the side surfaces of the column and carriage in the *x* and *y* directions. When the top surface of the column is excited by an impulse hammer in the *x*, *y*, and *z* directions, acceleration is detected by an accelerometer at each point. The FRF from the top of the column to the detection point of acceleration is measured. The mode shapes are measured by reading the compliance and phase of FRFs. The mode shape is normalized so that the amplitude may become 1 by dividing with maximum values of the compliance of each modes, and the amplitude in the *z* direction is scaled to be 200 times larger and that in the *y* direction is scaled to be 20 times larger. The mode shapes in the *x*, *y*, and *z* directions are shown in blue, green, and red, respectively.

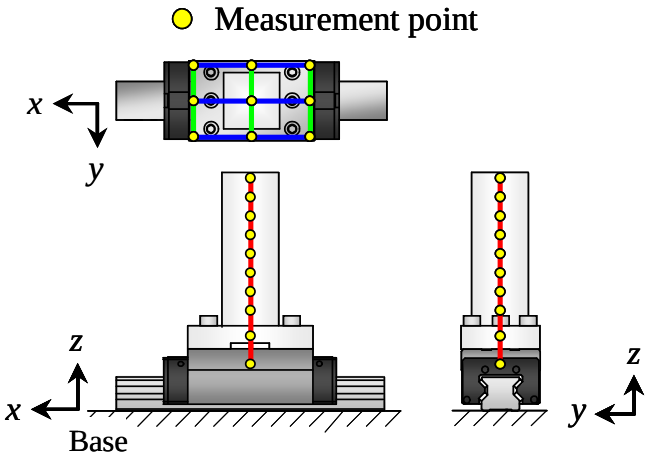

Fig. 7 Measurement point for experimental modal analysis

The mode shapes of the first and second modes when the column is excited in the *x* direction are shown in Fig. 8. Since the amplitude in the *y* direction is smaller than that in other directions, the mode shapes are shown on the *x*-*z* plane. In Fig. 8a, the motion of the carriage in the first mode is rotational about the *y* axis and translational in the *x* direction. The motion of the column appears to be similar to the rigid bar.

As shown in Fig. 8b, the motion of the carriage in the second mode is the rotational motion about the *y* axis, and the motion of the column appears to be similar to the bending

mode of a beam. The vibration amplitude of the translational motion of the carriage in the first mode is larger than that in the second mode. However, the vibration amplitude of the rotational motion of the carriage in the first mode is lower than that in the second mode. This means that the translational motion is predominant in the first mode, and the rotational motion is predominant in the second mode. Because the carriage is not fixed in the *x* direction, the carriage moves in the *x* direction in first mode. Thus, the vibration in the first mode is considered not to be caused by the elastic contact between the rollers and the raceways.

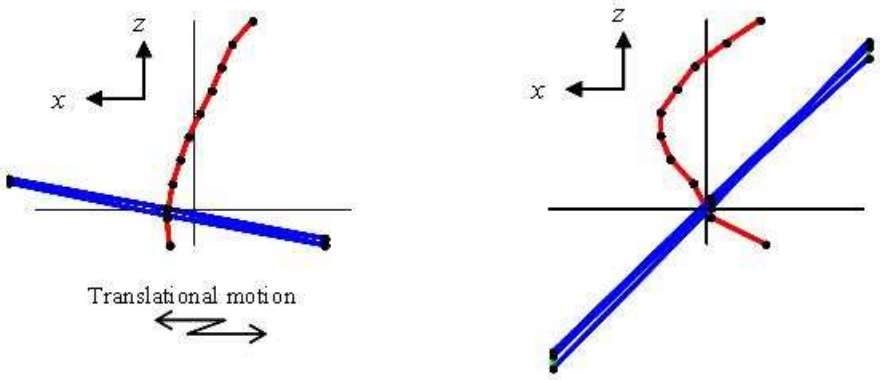

a) 1st mode b) 2nd mode

Fig. 8 Mode shape (Excitation direction: *x* direction)

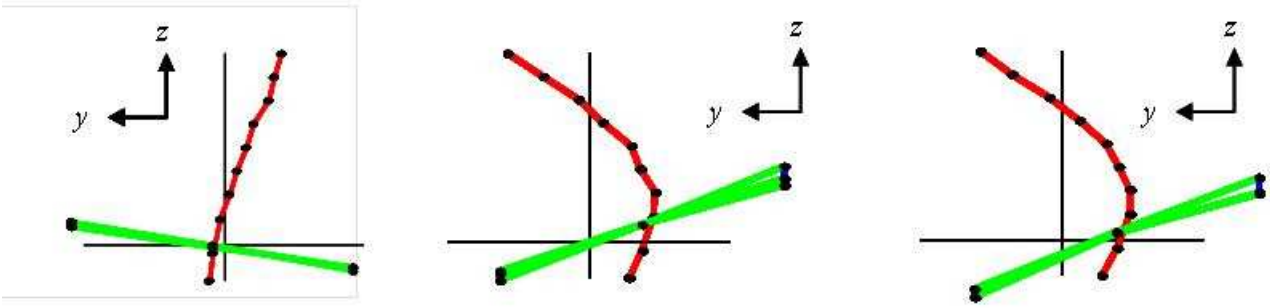

a) 1st mode b) 2nd mode c) 3rd mode

Fig. 9. Mode shape (Excitation direction: y direction)

Figure 9 shows the mode shapes of the first through third modes when the carriage is excited in the *y* direction. The mode shapes are displayed on the *y*-*z* plane because the vibration amplitude in the *x* direction is smaller than that in other directions. As shown in Fig. 9a, the motion of the carriage of the first mode is not only a translational motion in the *y* direction but also a rotational motion about the *x* axis, and the motion of the column appears to be similar to the rigid bar. Figure 9b shows the mode shape of the second mode. As shown in Fig. 9b, the motion of the carriage of the second mode is a translational motion in the *y* direction and an uplift motion in the *z* direction, and the motion of the column appears to be similar to the bending mode of a beam. The motion of the carriage of the third

mode (Fig. 9c) is similar to that of the second mode. Based on this result, the second and third modes are considered to be the same vibration mode.

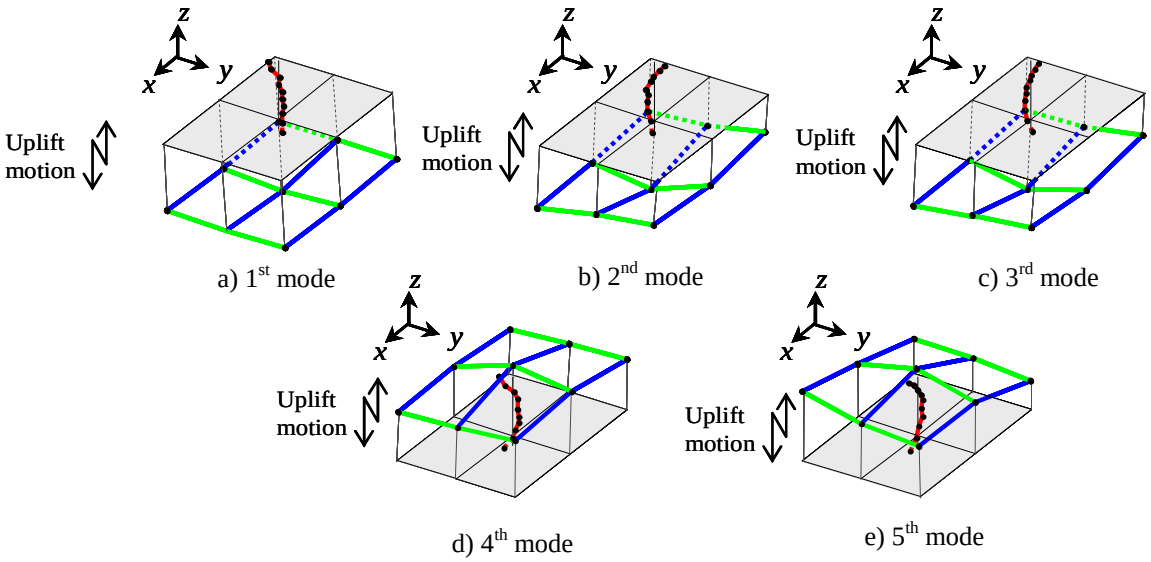

Fig. 10. Model shape (Excitation direct: z direction)

Figure 10 shows the mode shapes of the first through fifth modes when the carriage is excited in the *z* direction. The mode shape of the first mode is shown in Fig. 10a. The motion of the carriage is a translational motion in the *z* direction, and that of the column appears to be similar to the bending mode of a beam in the *x* direction. As shown in Figs. 10b and 10c, the motions of the carriage in the second and third modes are similar to that in the first mode. However, the motion of the column appears to be similar to the bending mode of a beam in the *y* direction. Therefore, the motions of the column of the second and third modes are different from that of the first mode.

Comparison of the mode shapes of the second and third modes indicates that these modes are similar, and these modes are considered the same vibration mode divided. The mode shapes of the fourth and fifth modes are shown in Figs. 10d and 10e, respectively. The phase of the FRF in the fourth and fifth modes is opposite that in the first through third modes. The motions of the carriage in the fourth and fifth modes are translational motions in the *z* direction, and motions of the column in the fourth and fifth modes appear to be similar to the bending mode of a beam in the *x* and *y* directions, respectively. Although the fourth and fifth modes appear in adjacent frequencies, the mode shapes differ. Therefore, the fourth and fifth modes are independent modes. As shown above, the vibration state of each mode became clear upon measuring the mode shape.

At the first mode in the *x* and *y* direction, the column vibrates as a rigid bar. Thus these first modes seem to be caused by the rigid body motion of the carriage. These modes are especially important when dealing in the vibration of a table of machine tools which is supported by linear rolling bearings. In higher modes in *x* and *y* directions, the column vibrates with bending mode. Hence the column influences on the dynamic characteristics in these modes.

4. EVALUATION OF DAMPING RATIO

The damping capacity of the linear rolling bearing for each vibration mode was evaluated based on the modal damping ratio calculated by the half power method. In this method, the modal damping ratio ζ is calculated using the frequencies f_1 and f_2 ($f_1 < f_2$), the amplitudes of which are 3 dB less than the maximum amplitude, and the resonance frequency f_n. The modal damping is calculated using the following equation:

$$\zeta = \frac{f_2 - f_1}{2 f_n} \tag{1}$$

The relationship between the modal damping ratio of each vibration mode and the resonance frequency is shown in Fig. 11, which shows that the modal damping ratio of each vibration mode is approximately 0.01. However, the modal damping ratio of the first mode in the *x* direction is noticeably higher than those of the other modes. Therefore, the reason the damping capacity in the first mode is higher than that in other modes is investigated by focusing on the vibration mode and the carriage mechanism.

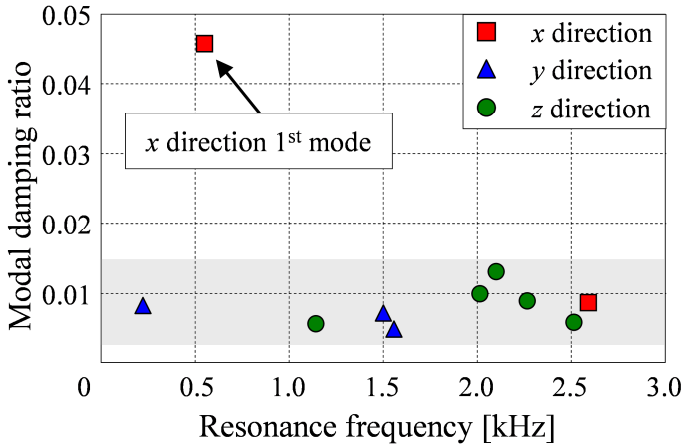

Fig. 11. Relationship between modal damping ratio and resonance frequency

5. GENERATION MECHANISM OF VIBRATION AND DAMPING

5.1. GENERATION MECHANISM OF VIBRATION

The motions of the carriage in the rotational direction, the *y* direction, and the *z* direction are fixed by the elastic contact component of the raceway and the rolling element. Since the elastic contact component acts as a spring, the carriage vibrates in the rotational direction, the *y* direction, and the *z* direction. The mode shapes shown in Figs. 9 and 10

indicate that the carriage vibrates in the *z*, *y*, and rotational directions when the carriage is excited in the *y* and *z* directions.

Hence, the vibration of the carriage was expected not to be generated in the *x* direction because the motion of the carriage is not fixed in the *x* direction. Nevertheless, the carriage vibrates in the *x* direction shown in Fig. 8a. Rolling friction is generated when the carriage moves in the *x* direction. In generally, the rolling friction force increases proportional to displacement in the microscopic displace region [12],[13]. This relation is called as the nonlinear spring characteristics of rolling friction. Since the displacement of the carriage generated by an impact excitation is very small, the friction force is considered to reveal the spring characteristics in the microscopic region, which cause the vibration of the carriage i n the *x* direction. As shown above, the carriage vibrates in the *x*, *y*, *z*, and rotational directions. However, the generation mechanism of the vibration in the *x* direction differs from that of the vibrations in other directions. In other words, the vibration of the carriage in the *x* direction is generated by friction, and the vibrations of the carriage in other directions are generated by the elastic contact component.

5.2. MECHANISM OF DAMPING GENERATION

Next, we investigate why the damping capacity of the first mode in the *x* direction is higher than that of the other modes. In the linear rolling bearing considered herein, the rollers are held in the carriage by a resin component having a flange, as shown in Fig. 12. Since the end face of the roller and the carriage come in contact, a large friction force is generated when the carriage vibrates in the *x* direction. Therefore, the damping capacity of the first mode in which the carriage vibrates in the *x* direction is larger than that of the other modes. The damping capacity of the carriage in the feed direction increases because a large friction force is generated. On the other hand, with the exception of that of the first mode in the *x* direction, vibration damping is generated by the micro-slip between the carriage and the rolling surface of the roller.

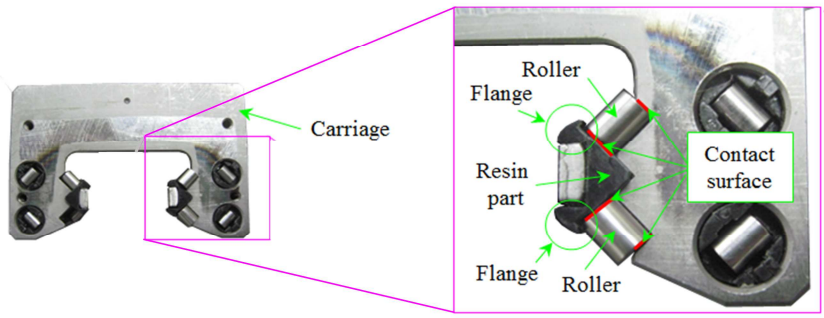

Fig. 12. Structure of a carriage for retaining rollers

However, the vibration damping generated by the micro-slip is less than that generated by the rolling friction because the carriage is fixed in all but the *x* direction.

6. NONLINEARITY OF DYNAMIC CHARACTERISTICS

The carriage of a linear rolling bearing is fixed elastically by the roller. Since the relationship of the elastic deformation of the carriage and the force is nonlinear, the dynamic characteristics of a linear rolling bearing vary with the magnitude of the exciting force. In order to investigate the influence of the nonlinearity of the carriage, the FRF of the linear rolling bearing was measured for forces of three different magnitudes. Since the impulse response method was used, the magnitude of the excitation force could not be controlled.

In order to qualitatively investigate the influence of the nonlinearity, small, moderate, and large forces were applied. Fig. 13 shows a Nyquist diagram of the first and second modes obtained as for the three excitation forces. As shown in Fig. 13, the diameter of the circle differs according to the magnitude of the excitation force, which indicates that the damping capacity decreases as the diameter of circle increases. Thus, the damping capacity of a linear rolling bearing changes with the magnitude of the excitation force. Fig. 14 shows Nyquist diagrams of the first through third modes in the *y* direction obtained for the three excitation forces.

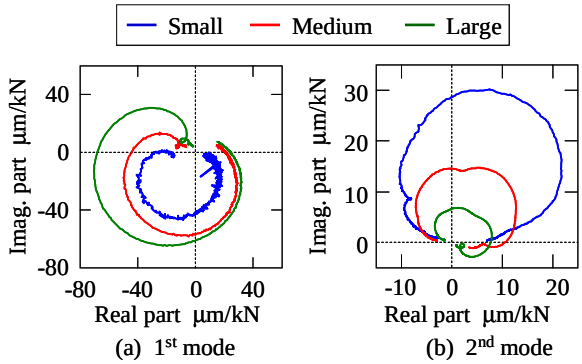

Fig. 13. Influence of excitation force
(Excitation direction: *x* direction)

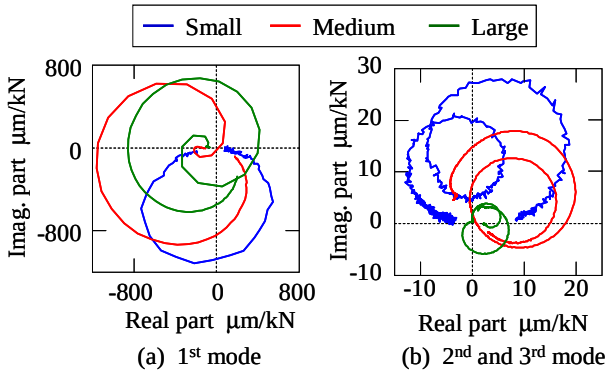

Fig. 14. Influence of excitation force
(Excitation direction: *y* direction)

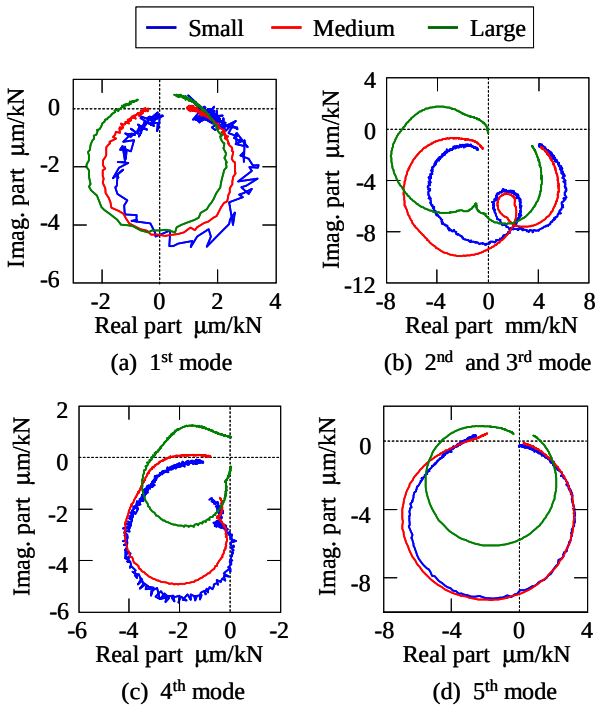

Fig. 15. Influence of excitation force
(Excitation direction: *z* direction)

Fig. 15 Also shows Nyquist diagrams of the first through fifth modes in the *z* direction obtained for the three excitation forces. The diameter and shape of the Nyquist diagram changes with the magnitude of the excitation force. Then, the resonance frequency and the magnitude of the excitation force are examined. Fig. 16 shows the relationship between the resonance frequency and the magnitude of the excitation force. As shown in Fig. 16, the resonance frequency decreases as the magnitude of excitation force increases. This figure indicates that there is nonlinearity in the dynamic characteristics, including the stiffness and damping capacity. Moreover, the magnitude of the excitation force influences the resonance frequency of the first mode in the *x* direction more than those in other modes. In general, the stiffness of rolling friction force in the microscopic displacement region decreases with increasing the displacement [12],[13]. This displacement dependency of rolling friction causes the large decrement of resonance frequency at the first mode in the *x* direction.

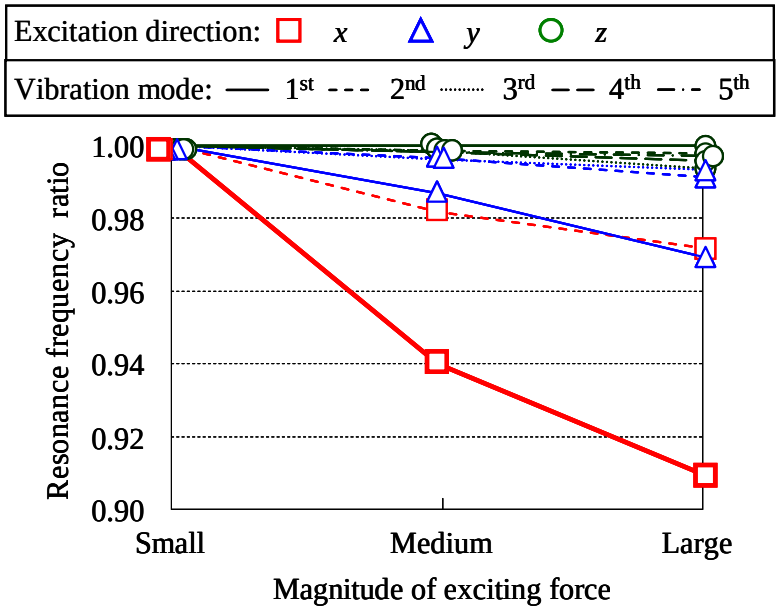

Fig. 16. Influence of magnitude of excitation force

7. CONCLUSION

The present paper proposes a method for evaluating the damping capacity of a single linear rolling bearing subjected to a bending moment and a radial force. The column used for measurement was fixed to the top surface of the carriage of a linear rolling bearing. The bending moment was applied to the carriage when the top of the column was excited. The magnitude of the excitation force was varied in order to investigate the influence of the nonlinearity of the linear rolling bearing.

The conclusions of the present study are summarized as follows.

(1) From the evaluation of the results, the damping capacity of the vibration mode for which the carriage moves in the *x* direction is the greatest. Moreover, the influence of the magnitude of the excitation force on the resonance frequency of the first mode in the *x* direction is greater than in other modes.
(2) The vibration in the *x* direction might be caused by nonlinear friction in a microscopic region consisting of a few micrometers. Since the end face of the roller and the carriage come into contact, high friction damping is generated in the *x* direction.
(3) The nonlinearity of the linear rolling bearing influences its dynamic characteristics. The resonance frequencies decrease as the magnitude of the excitation force increases.

The damping ratio is influenced by the column mass. The damping coefficient should be calculated to exclude the influence of the column mass. And the dynamic characteristics are sensitively changed by the magnitude of the excitation force. Hence the force dependency of dynamic characteristics including damping coefficient will be investigated in the future work.

REFERENCES

[1] ISO 14728-1, 2004, *Rolling bearings – linear motion rolling bearings - Part 1: Dynamic load ratings and rating life*.
[2] SHIMIZU S., SHARMA C.S., SHIRAI T., 2002, *Life prediction for linear rolling element bearings: A new approach to reliable life assessment*, Journal of Tribology, 124/1, 121 – 128.
[3] SHIMIZU S., SHIMODA H., TOSHA K., 2008, *Study on the life distribution and reliability of roller-based linear bearing*, tribology transactions, 51/4, 446 – 453.
[4] OHTA H., HAYASHI E., 2000, *Vibration of linear guideway type recirculating linear ball bearings*, Journal of Sound and Vibration, 235/5, 847 – 861.
[5] YI Y-S., KIM Y.Y.,CHOI J.S., YOO J., LEE. D.J., LEE S.W., LEE S.J., 2008, *Dynamic analysis of a linear motion guide having rolling elements for precision positioning devices*, Journal of Mechanical Science and Technology, 22, 50 – 60.
[6] BODE H., 1990, *Rolling-bearing mounted linear guiding unit and damping unit*, INA Walzlager Schaeffler KG, US Patent, No.4968155.
[7] RAHMAN M., MANSUR M.A., LEE L.K., LUM J.K., 2001, *Development of a polymer impregnated concrete damping carriage for linear guideways for machine tools*, International Journal of Machine Tools & Manufacture, 41, 431 – 441.
[8] POWALKA B., OKULIK T., 2010, *Influence of application of special casting compound on dynamic characteristics of the guideway system*, Journal of Machine Engineering, 10/2, 71 – 81.
[9] RUSSELL T. GILMAN INC., 2001, *Gilman linear guide slides catalog*, 5.
[10] NSK, *Damping in linear ball guide*, http://www.jp.nsk.com/services/pm_techreport/report40.html (in Japanese).
[11] BRECHER C., FEY M., BAUMLER S., 2012, *Identification method for damping parameters of roller linear guides*, Production Engineering, 6, 505 – 512.
[12] AL-BENDER F., SYMENS W., SWEVERS J., VAN BRUSSEL H., 2004, *Theoretical analysis of the dynamic behavior of hysteresis elements in mechanical systems*, International Journal of Non-Linear Mechanics, 39/10, 1721 – 1735.
[13] TJAHJOWIDODO T., 2012, *Theoretical analysis of the dynamic behavior of presliding rolling friction via skeleton technique*, Mechanical Systems and Signal Processing, 29, 296 – 309.